ELSEVIER

Journal of Nuclear Materials 280 (2000) 1–17

journal of nuclear materials

www.elsevier.nl/locate/jnucmat

Estimates of helium gas release in $^{238}PuO_2$ fuel particles for radioisotope heat sources and heater units

Mohamed S. El-Genk *, Jean-Michel Tournier

Department of Chemical and Nuclear Engineering, School of Engineering, Institute for Space and Nuclear Power Studies, The University of New Mexico, Farris Engineering Ctr. Room 237, Albuquerque, NM 87131-1341, USA

Received 15 December 1999; accepted 7 March 2000

Abstract

Release data of noble gases (Xe and Kr) from small-grain (7–40 μm), large-grain (⩾ 300 μm), and monocrystal UO_2 fuel particles, during isothermal irradiation up to 6.4 at.% and 2030 K are reviewed and their applicability to estimate helium release from $^{238}PuO_2$ fuel particles (⩾ 300 μm in diameter) is examined. Coated $^{238}PuO_2$ particles have recently been proposed for use in radioisotope power systems and heater units employed in planetary exploration missions. These fuel particles are intentionally sized and designed to prevent any adverse radiological effect and retain the helium gas generated by the radioactive decay of ^{238}Pu, a desired feature for some planetary missions. Results suggest that helium release from large-grain (⩾ 300 μm) particles of K could be <7% at 1723 K, <0.6% at 1042 K, and even less for polycrystalline particles fabricated using sol–gel processes. Results also suggest that helium release from small-grain plutonia particles at 1723 K could be >80% but less than 7% at 1042 K, which is in general agreement with the experiments conducted at Los Alamos National Laboratory more than two decades ago. In these experiments, the helium gas release from small-grain (7–40 μm) $^{238}PuO_2$ fuel pellets has been measured during steady-state heating at temperatures up to 1886 K and ramp heating to 1723 K.

PACS: 29.25.R; 51.20.+d; 81.05.Rm

1. Introduction

As part of an initiative to develop new fuel forms for radioisotope power systems and heater units employed in space planetary exploration missions, coated $^{238}PuO_2$ fuel kernels have recently been proposed [1,2]. The concept and the early technology of coated UO_2, UC, and (U, Zr)C fuel particles have been developed during the ROVER and the NERVA Nuclear Rocket Programs, in the 1960s and early 1970s [3–6]. These programs were carried out at Los Alamos National Laboratory, in collaboration with Atomic International and Westinghouse Electric Company. The proposed coated $^{238}PuO_2$ fuel particles also draw on the vast and proven fabrication technology of UO_2 and (U, Pu)O_2 TRISO fuel particles in high temperature gas-cooled reactors (HTGRs) [7–11].

The attractive features of the coated fuel particles in fission reactors are their ability to operate at high temperatures and achieve high burnup (>30 at.%), with little concern about fuel swelling and fission products release. The primary coating of these fuel particles (SiC for operating at <1300 K or ZrC for operating at higher temperatures) serves as a pressure vessel for containing the fission products and constraining fuel swelling during irradiation [7–11]. The fuel kernel (300–1200 μm in diameter) could be fabricated using powder metallurgy techniques [7,12,13], bed and plasma melting processes [14–16], or sol–gel techniques [8,17–19]. Unlike powder metallurgy, the sol–gel and thermal plasma techniques do not involve any milling and grinding and, hence, generate little, if any, post-fabrication radioactive solid waste. The literature on the fabrication and material properties of coated fuel particles has recently been reviewed and documented [20].

* Corresponding author. Tel.: +1-505-277 5442; fax: +1-505-277 2814.

E-mail address: mgenk@unm.edu (M.S. El-Genk).

0022-3115/00/$ - see front matter
PII: S0022-3115(00)00036-2

The coated $^{238}PuO_2$ fuel particles, proposed for potential use in radioisotope heater units (RHUs) and radioisotope power systems (RPSs) [1,2], are intentionally sized ($\geqslant 300$ μm in diameter) to prevent any adverse radiological effect; they are non-respirable and non-inhalable, and if ingested, would simply be excreted with no radiological effect [2]. These coated plutonia ($^{238}PuO_2$) particles are also designed to retain the helium gas generated by the radioactive decay of ^{238}Pu. Some of the space missions that employ planetary probes for in situ analysis of surface materials require that the He gas be fully retained, in order to avoid contaminating the environment and skewing sensitive measurements [21]. Such an option is not attainable using the current RHU and the general purpose heat source (GPHS) designs [1]. The coated particles fuel form can be fabricated in different shapes, sizes, and power densities. For examples, coated particles fuel dispersed in a graphite matrix could be made into various shapes of solid compacts, or used in the form of a heating tape or paint for a variety of space applications. This design and fabrication flexibility is a desirable feature for scientific probes requiring both thermal and electric power and in which the RHU can be fabricated to optimize the design, operation, and the functionality of the probe.

The coated plutonia fuel particles proposed for use in RPSs and RHUs consist of a fuel kernel ($\geqslant 300$ μm in diameter) having a thin (5 μm) Pyrolytic Graphite (PyC) inner coating and a strong ZrC outer coating (see Fig. 1). The thickness of the ZrC coating depends on the fuel kernel diameter and the internal pressure of the helium gas released from the fuel kernel [2]. The coated particles fuel compact (CPFC) in a pellet form could be used to develop high specific power RHUs, utilizing the current fine weave pierced fabric (FWPF) aeroshell [22,23]. It has recently been shown that replacing the $^{238}PuO_2$ pellet, the Pt-alloy cladding, and the inner insulation graphite sleeve in a light weight RHU (LWRHU) with CPFC increases the thermal output from ~1.0 to 1.54, 2.40 and 2.52 W, when assuming 100%, 10% and 5% helium release, respectively [2]. Such high thermal powers were possible at essentially the same LWRHU mass (~40 g) and conservatively assuming a pre-launch storage time of 10 yr and a fuel temperature of 1723 K. This temperature is the predicted maximum value during an accidental re-entry heating pulse of the LWRHU [22].

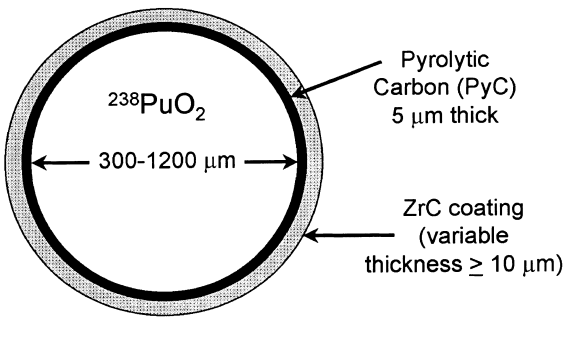

Fig. 1. Coated plutonia fuel particle.

The higher the release fraction of He, the thicker is the ZrC coating of the $^{238}PuO_2$ kernels needed to accommodate the internal gas pressure, reducing the fuel loading in CPFC. Therefore, it is important to determine the He gas release in coated plutonia fuel kernels as a function of temperature and storage time before launch, in order to maximize the fuel loading in the CPFC. In addition to the storage time and temperature, the He gas release depends on the grain size and the fuel microstructure (granular or polycrystalline). Therefore, it is also important to examine the effect of the fuel microstructure on the helium gas release in the coated plutonia particles.

During FY99, an exploratory effort sponsored by the Department of Energy was initiated to investigate the potential of the $^{238}PuO_2$ CPFC for use in RHUs and address the fabrication and performance issues. This effort was performed jointly by Sandia National Laboratories, Sholtis Engineering and Safety Consulting, and the University of New Mexico's Institute for Space and Nuclear Power Studies. The specific tasks investigated were to:

1. review the fabrication technologies of coated plutonia fuel particles;
2. review the release mechanisms of helium gas in small-grain (7–40 μm) plutonia pellets in GPHSs and LWRHUs, and examine the applicability of these mechanisms to the He release from large-grain ($\geqslant 300$ μm) and polycrystalline fuel kernels;
3. review the spectrum of credible launch and reentry accident environments that the coated particle fuel could potentially experience. Based on this review, design and functional requirements for coated particle fuel were established;
4. develop a design and performance model of coated fuel particles to investigate the impact of using single-size and binary-size CPFC on the thermal power level of a RHU. Also quantify the effects on the RHU thermal power of the helium gas release, fuel temperature, and storage time before launch; and
5. identify future research and testing needs to confirm the coated particle fuel's potential operation and safety promise [24].

This paper reviewed the release data of noble gases (Xe and Kr) in small-grain (7–40 μm), large-grain ($\geqslant 300$ μm), and monocrystal UO_2 fuel particles, irradiated at constant temperatures up to 2030 K and a burnup up to 6.4 at.% [21–25], and examined their applicability to estimate the helium release from $^{238}PuO_2$ fuel particles having the same microstructure. The

measured release fractions of the Xe and Kr isotopes for the small-grain UO_2 fuel particles are compared with the reported helium gas release data by Los Alamos National Laboratory for small-grain (7–40 μm) plutonia pellets, currently being used in GPHSs and RHUs. These He gas release measurements were from small-grain (7–40 μm) $^{238}PuO_2$ fuel pellets during steady-state at temperatures up to 1886 K and ramp heating to 1723 K.

2. Basic microstructures of fuel kernels

There are two basic microstructures of oxide fuel kernels (Fig. 2): (a) *the granular microstructure* obtained by powder metallurgy processes [7,12,13]; and (b) *the polycrystalline microstructure* obtained by the sol–gel [8,17–19] and melting processes [14–16]. A granular fuel kernel consists of a number of polycrystalline grains of almost the same size (typically 7–40 μm). Common grain boundaries are developed during sintering of the kernels at high pressure and temperature. This process also controls the as-fabricated porosity in the fuel and at the triple interface of the grains to accommodate the released fission gases during operation in nuclear reactors. The as-fabricated porosity of a typical oxide fuel kernel ranges from 5% to 15%.

2.1. Granular fuel kernels

Granular fuel kernels are fabricated using the binderless agglomeration process [7,12,13]. This process produces highly spherical and virtually monosized oxide fuel kernels in the range 200–1000 μm in diameter and with a porosity between 5% and 20% (see Fig. 2(a)). Green spheroids are initially prepared from ceramic-grade, UO_2 or mixed oxide powder, having a specific surface area of 2–4 m^2/g. The fuel powder is mixed (using ball milling) with proprietary carbon blacks, having a specific surface area of 15–30 m^2/g. The resulting powder is granulated to form seeds, which are then grown to the desired kernel size in a vibrating pan fed with fresh fuel powder. The fuel green spheroids, or 'seeds' are formed by the simple action of gyrating the fine sub-micron fuel powder in a bowl. These seeds have a size distribution in the range between 150 and 200 μm. Fine fuel powder is then added at a controlled rate to the charge of seeds, while being continuously gyrated in a bowl. The fuel oxide/C 'green' particles are then spheroidized in a rotary sieve or planetary mill [12,13].

Porous oxide fuel kernels are fabricated from the green particles using a two-stage heat treatment process to control the fuel's as-fabricated porosity and stoichiometry. First, the green fuel microspheres are consolidated by sintering in carbon monoxide at 1923 K to prevent carbide formation. The sintered particles are then decarbonized in a flowing CO/CO_2 at 1573 K in a continuous furnace. The removal of the carbon leaves the desired porosity within the fuel microspheres (Fig. 2(a)) [7,12,13].

2.2. Polycrystalline fuel kernels

Polycrystalline fuel kernels fabricated using sol–gel techniques [8,17–19] could have diameters as large as 1200 μm. These techniques do not require milling or grinding (as during the fabrication of granular fuel by powder metallurgy), thus generate very little, if any, radioactive dust or aerosols. Liquid wastes, however, may be produced in the sol–gel processes, depending upon the efficiency of recycling the used chemicals. These all wet chemical processes use solutions or sols (or suspensions) of fissile or fertile materials dispersed in the form of uniform liquid (gel-like) droplets. The spherical shape of the droplets is retained in the gelation process (using water or ammonia extraction) involving either precipitation or dehydration reactions. The gelled fuel microspheres, which have an almost perfect sphericity, are then washed, dried, and fired at high temperature to remove water and volatile additives and sinter the spheres to the desired density and fuel stoichiometry. The sintered fuel kernels have a polycrystalline fuel

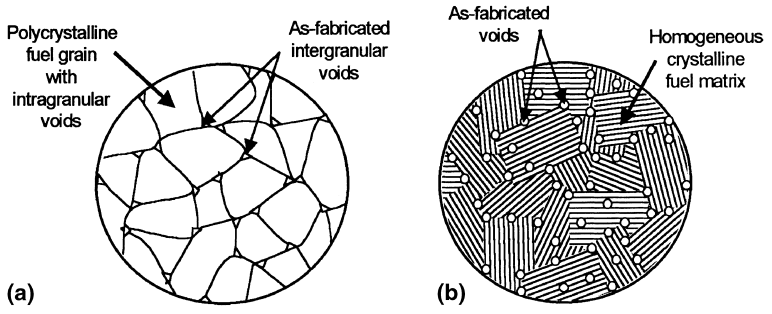

Fig. 2. Basic fuel microstructures for coated fuel particles: (a) granular fuel kernel fabricated using powder metallurgy; (b) polycrystalline fuel kernel fabricated using sol–gel techniques.

structure with tiny, intragranular voids (<1 μm in diameter) (see Fig. 2(b)).

The amount of porosity in the sol–gel, oxide fuel kernels (5–20%) is controlled during the sintering process. Thus, for helium release, the polycrystalline fuel particles (Fig. 2(b)) may be regarded as a single grain of the kernel diameter, with as-fabricated intragranular porosity made of tiny pores dispersed throughout the fuel kernel. Bed melting and thermal plasma processes could also be used to produce spherical oxide fuel kernels. However, these techniques do not exhibit high reproducibility nor allow for close control of fuel volume porosity [14–16]. The release mechanisms of radioactive fission gases and volatile fission products in granular UO_2, mixed-oxide fuels and of helium in granular plutonia fuel is discussed next.

3. Gas release mechanisms in UO_2, $(U, Pu)O_2$ and PuO_2 fuels

There are strong similarities between the release mechanisms of noble gases in granular oxide and mixed-oxide fuels and those of helium in granular $^{238}PuO_2$, but also there are some differences. For example, the restructuring and cracking of UO_2 fuel, which occur during irradiation in fission reactors, depending on the fuel pellet diameter and fission power density, and influence the fission gas release, do not exist in $^{238}PuO_2$ fuel. In fission reactors, the power density in the fuel pellets is orders of magnitude higher than that by natural radioactive decay of ^{238}Pu in plutonia pellets. When such high power density is combined with the inherently low thermal conductivity of the fuel material, fuel pellets in fission reactors develop a steep, parabolic radial temperature distribution and significantly higher fuel temperatures, particularly near the pellet centerline. The combination of high temperature and radial temperature gradient causes significant cracking and restructuring of oxide and mixed oxide fuel in fission reactor [30]. Also, the induced defects in UO_2 and mixed oxide fuel associated with the uranium recoil and the knock-on atom displacement caused by the fission fragment would affect the fission gas release, but are non-existent in $^{238}PuO_2$ fuel. However, owing to the similar ceramic nature of the oxide and mixed oxide fuel used in fission reactors and plutonia fuel, for the same temperature, as-fabricated porosity, and grain size, the noble gas release mechanisms could be quite similar. Particularly at high temperatures (>900 K), the micro-cracking, the irradiation damage caused by fission fragments, and the knock-on atom defects in oxide and mixed oxide fuel tend to partially recover. This argument is investigated in this paper as it pertains to the release of noble fission gases in UO_2 fuel particles at almost uniform temperatures and the helium gas release in $^{238}PuO_2$ fuel.

The processes by which the generated gas atoms nucleate into tiny bubbles within the fuel grains, and by which the bubbles grow, diffuse, and eventually coalesce at the grain boundaries are extremely complex [30–32]. The fuel temperature, however, provides a useful index for determining the prevailing release mechanisms and the rate of gas release from granular fuel.

3.1. Effect of temperature on gas release

The release mechanisms of the gases generated either by fission in uniformly heated UO_2 fuel particles or by radioactive decay of ^{238}Pu in radioisotope heat sources can be summarized as follows [26–28]:

(a) *At low temperatures* (<900 K), *the generated gas atoms initially dissolve in the fuel matrix or form tiny clusters*. Experimental observations have shown that most of the gases remain in solution in the fuel matrix [30,33–35]. As the gas atoms supersaturate the fuel matrix, they form tiny intragranular bubbles, less than 1 μm in diameter (Fig. 3(a)). Therefore, at such low temperatures, the generated gas is constrained by the geometrical surface area available for release and its low diffusion coefficient in the fuel matrix. The intragranular gas atoms, through recurrent precipitation and/or resolution events, undergo long-range diffusion through the fuel grains and are ultimately captured in the grain boundary pores or at the transgranular free surfaces in the grains. So long as the generated gas remains trapped within the fuel grains, only a negligible fraction is released by diffusion. Therefore, the larger are the as-fabricated fuel grains, the longer it takes the generated gas atoms to diffuse to the grain boundaries and the fuel surface, resulting in lower release rates. At fuel temperatures up to ~1100 K, the probability that the generated gases would be trapped within the fuel matrix and at the grain boundaries is large; only gases generated near the fuel surface may escape. Thus, the release fraction at such low fuel temperatures is typically very low, and solely dependent on the available surface area for gas release and the potential development of tiny cracks or open porosity near the fuel pellet surface.

(b) *At intermediate temperatures* (1100–1400 K), *the fuel grains slowly grow in size*. The convex and concave grain boundaries move inward and outward, respectively (Fig. 3(b)), sweeping the gas atoms and tiny intragranular bubbles to the grain boundaries where they are irreversibly trapped (Fig. 3(a)). The difference between the partial pressure in the tiny intragranular bubbles and that in the larger bubbles at the grain boundaries provides the concentration gradient for further gas diffusion, over time, from the fuel matrix to the

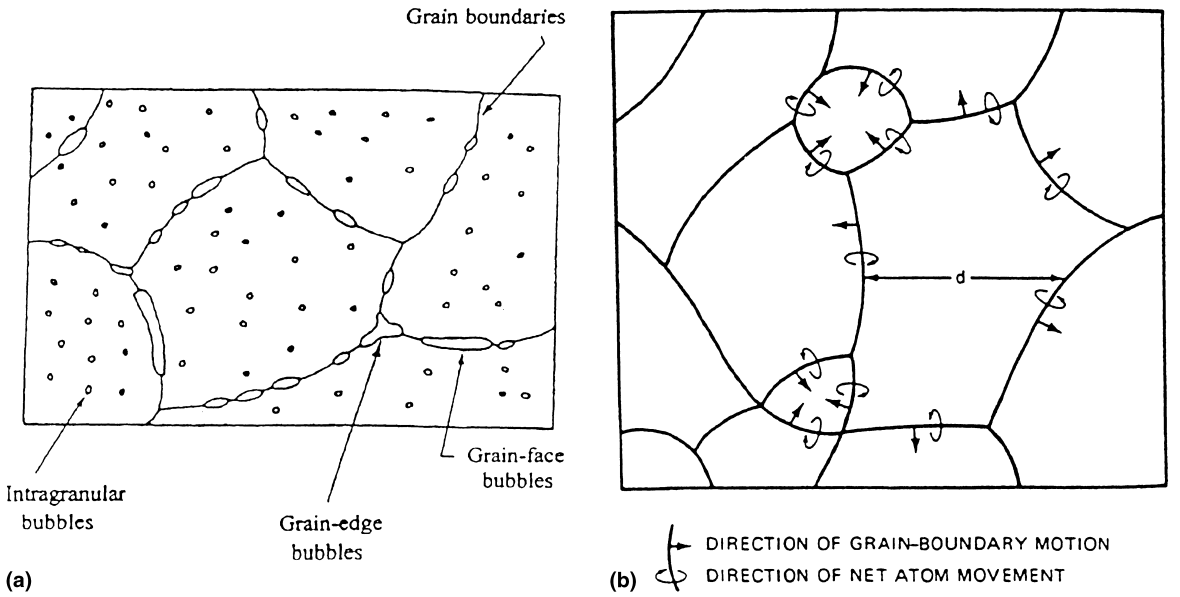

Fig. 3. Schematic cross-sections of granular fuel with generated gas [30]: (a) intragranular and intergranular gas bubbles; (b) grain boundary motion during grain growth.

grain boundaries. At these temperatures, gas is released from the grain boundary bubbles by diffusion along the grain boundaries, to the open porosity in the fuel.

(c) *At temperatures of* ~1200–1600 K*, as the intergranular bubbles grow by capturing additional gas atoms and intragranular bubbles, they coalesce into larger elongated bubbles*. With time and/or an increase in the fuel temperature, the growth and expansion of bubbles at the grain boundaries cause the formation of open porosity or tiny 'tunnels' for the gas release. This process, which occurs as the grain boundary strength decreases below the transgranular strength [36], is characterized typically by a burst release of the gases trapped at the grain boundaries [28–34]. The gradual increase in the open porosity at the grain boundaries with temperature, or with time at temperature, increases the gas release rate from the fuel. The formation of open porosity networks in the fuel pellet is almost complete as the fuel temperature approaches 1500 K, at which the release rate of the generated gas is no longer constrained by the surface area available.

(d) *At temperatures* >1600 K, *the increased mobility and mass diffusion of the intragranular bubbles and gas atoms increase the release rate of the newly generated gases*. The gas diffuses through the fuel grains to the large surface area provided by the open porosity networks, where it is readily released. Therefore, at such fuel temperatures, the increase in the gas release rate is related essentially to the increase in the atomic and volume diffusion through the fuel grains, since the surface area available for release remains unchanged.

3.2. Gas release mechanisms

In summary, the release of noble gases generated by fission in UO_2 fuel particles held at almost uniform temperatures or by radioactive decay in $^{238}PuO_2$ could be similar and occur by the following four sequential mechanisms [30–32,34–37].

Atomic diffusion near the surface of the fuel pellet or particles when the fuel temperature is <900 K. The release fraction in this case is typically very low, since it is limited by the available surface area for release and the relatively low diffusion coefficient of the gases in the fuel matrix. Therefore, at such low fuel temperatures, most of the generated gases remain within the fuel grains and the gas release is nil [33–37].

Accumulation in intergranular gas bubbles. Grain boundary bubbles form due to the enhanced mobility of the tiny intragranular gas bubbles and the growth of fuel grains at temperatures ~1150 K or higher. At such temperatures, some open porosity may form at the grain boundaries, resulting in a higher gas release. The gas release fraction, however, remains well below 10%, due to the limited surface area for gas release.

Formation of open porosity networks, which occurs at fuel temperatures of ~1150–1600 K. At these high temperatures, the gas accumulated in the grain boundary bubbles is released through the forming open pores along the grain boundaries or open tunnels connecting the pores at the triple points of the fuel grains.

Atomic and volume diffusion to the open pores in the fuel. This mechanism, which is dominant at fuel

temperatures in excess of 1600 K, depends solely on the fuel temperature since the gas release is no longer limited by the available surface area for release. At these temperatures, the open porosity at the grain boundaries and open tunnel networks in the fuel are fully accessible for the release of the generated gas from the fuel grains.

These mechanisms have been confirmed by the experimental data generated at Los Alamos National Laboratory for the release of helium gas from GPHS and RHU plutonia fuel pellets. The release fraction of He was measured as a function of storage temperature and time during both steady-state and transient re-entry heating conditions [16,33–35,37,38]. The results described next illustrate the strong dependence of the release fraction of He on the as-fabricated grain size and the temperature of the fuel.

4. Helium gas release from small-grain plutonia fuel pellets and test samples

Results of helium release experiments from granular plutonia pellets (7–40 μm grain size) have indicated that transient heating increases the release rate, but that the release fraction depends on the temperature reached during the transient [37,38]. Similar release fractions of helium were reported at the same temperatures during steady-state heating experiments of granular pellets and smaller samples [33,34]. The experimental results also showed that He release below 900 K was nil. However, increasing the grain size decreased the He release fraction at the same fuel temperature.

The reported experimental data on helium gas release from granular $^{238}PuO_2$ fuel pellets covered grain sizes from 7–50 μm and storage times from a few months up to ~8 yr. These experiments investigated the effects of the fuel storage time and temperature and the temperature during both isothermal and ramp heating on the fuel microstructure and the helium gas release fraction. Most He release results were consistent with those obtained in the very comprehensive study of Peterson et al. [37]. The helium release data were fitted using the equivalent-sphere diffusion model to estimate the effective diffusion coefficient, $D' = D/a^2$, as a function of fuel temperature and ramp rate. The $^{238}PuO_2$ fuel samples, whose results are shown in Fig. 4, had 84.4% TD, an average grain size of 30–50 μm, and were heated slowly to 1300 K. The samples' temperature was then increased from 1300 to 1773 K in 125 s, at a ramp rate of 227 K/min [37]. The reported release mechanisms are indicated in Fig. 4. The temperatures corresponding to the transition points in the figure were almost the same for all samples ($T_a \approx 900$ K, $T_b \approx 1150$ K, $T_c \approx 1450$ K, $T_d \approx 1650$ K) to within ±75 K. The helium release mechanisms for small-grain plutonia fuel were in agreement with the release mechanisms discussed earlier

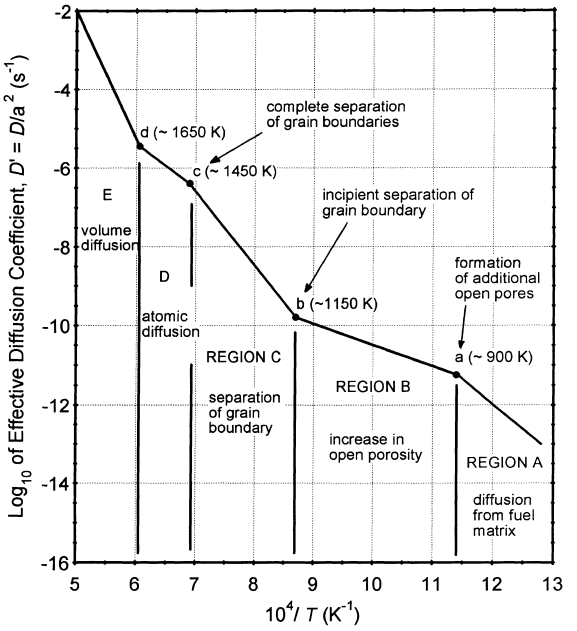

Fig. 4. Helium gas release in small plutonia fuel samples (30–50 μm grains, 7-month-old) heated slowly to 1300 K then ramped at a heating rate of 227 K/min from 1300 to 1773 K [37].

and with the theory of fission gas release to be discussed later in this paper. The data showed that D' was independent of the heating rate, but rather depended on the available surface area for helium release (or induced fuel restructuring), the fuel temperature reached, and the initial helium inventory [37].

4.1. Helium gas release regions/mechanisms

The helium release data can be classified into the following regions, each representing a dominant release mechanism from the granular plutonia fuel, namely (Fig. 4):

Region A, in which the dominant He release mechanism was atomic diffusion, occurred at relatively low temperatures $T < T_a$ (where $T_a \sim 900$ K). At these temperatures, the helium release fraction was very small (<1%) and the generated helium atoms were retained within the fuel grains. The concentration of helium in the fuel samples was essentially uniform, except near the samples' surface where only the helium atoms generated within one range (~12 μm) of the 5-MeV alpha particles from the surface were released.

Region B, in which the He gas atoms released from the fuel matrix were accumulated in growing intergranular gas bubbles in the pores at the triple points of the fuel grains, spanned somewhat higher temperatures, $T_a < T < T_b$ where $T_b \sim 1150$ K). The helium gas release at these temperatures is higher than in Region A. It is

characterized by trapping of diffusing helium atoms and tiny intragranular bubbles in the grain boundary bubbles. The growth and coalescence of the latter result in the formation of open pores along the grain boundaries, enhancing the helium release. The helium release also occurs by atomic diffusion along the grain boundaries to the outer surface of the fuel (Fig. 4).

Region C, in which separation of the grain boundaries and formation of networks of open tunnels in the fuel occurred, spanned the temperature range $T_b < T < T_c$ where $T_c \sim 1450$ K). At these temperatures, the grain boundary strength dropped below the transgranular strength of the fuel [36]. Thus, the growing intergranular bubbles gradually caused separation at the grain boundaries, increasing the helium release from the fuel grains through the resulting open porosity. The formation of intergranular open porosity was almost complete as the fuel temperature reached $T_c \sim 1450$ K, at which the helium atoms diffusing to and reaching the grain boundary are readily released (Fig. 4).

Region D, in which the dominant release mechanism of helium gas from the fuel grains was atomic diffusion, spanned the temperature range $T_c < T < T_d$ where $T_d \sim 1650$ K). At such high fuel temperatures, the increased mobility of the helium atoms in the fuel grain increased their diffusion to the open porosity at the grain boundaries and to the surface of the fuel pellet (Fig. 4).

Region E, in which the dominant release mechanism was volume diffusion, occurred at fuel temperatures $> T_d \sim 1650$ K. In addition to atomic diffusion, the helium release increased because of the high mobility and diffusion of the tiny intragranular helium bubbles to the open porosity at the grain boundaries (Fig. 4).

These release mechanisms of helium in granular plutonia fuel are essentially the same as those described earlier for noble fission gases in oxide or mixed-oxide fuel particles irradiated at uniform temperature. The effective size of the release unit (d) in granular oxide and plutonia fuels can be predicted by the equivalent-sphere diffusion model [30]. Since the effective diffusion coefficient, D' is inversely proportional to the square of the size of the release unit or average fuel grain ($D' = 4D/d^2$, where D is the mass diffusion coefficient), large-grain fuel will retain more of the generated gas than small-grain fuel. In small-grain fuel, the temperatures for incipient formation of open porosity by the coalescence of the grain boundary bubbles, T_a, and the separation of the grain boundaries, T_b (Fig. 4), are shifted to higher values. Owing to the longer grain boundaries in small-grain fuel, more helium would have to be released from the fuel grains to form intergranular bubbles and achieve the appropriate gas pressure to form open porosity at the grain boundaries. In addition, in small-grain fuel, Regions D and E in Fig. 4 become indistinguishable. A distinction between the contributions of atomic and volume diffusion becomes difficult because of the short diffusion distance of helium in the small fuel grains.

The following sections summarize the helium release measurements for small-grain (7–40 μm), plutonia fuel pellets and particles in the experiments performed at Los Alamos National Laboratories more than two decades ago [33,34,38].

4.2. Helium release measurements in isothermal heating experiments

Mulford and Mueller [33] have measured the helium release rates from plutonia microspheres fabricated using thermal plasma and from 6.4-mm right-cylindrical plutonia fuel pellets at constant temperatures. The fuel pellets were cold-pressed and fired for 6 h at 1923 K in a CO_2 atmosphere, weighed between 1.8 and 2.3 g, and had 87–88% TD. About 100 days had elapsed between the pellet sintering and the helium release measurements. The fuel samples were heated to the desired temperature as rapidly as possible, and then held at temperature for about 24 h, while the helium release rate was monitored continuously. The measured isothermal He release fractions from the LWRHU fuel pellets are shown in Fig. 5 versus the square root of time, at different fuel temperatures. The higher the fuel temperature, the higher the asymptotic fractional release of the helium and the faster it was reached. At 1749 K, the helium release fraction reached an asymptotic value of 0.8 after ~2.7 h. A helium release fraction of 0.57 was observed after 24 h at 1637 K, 1.2 h at 1749 K, and 20 min at 1886 K (Fig. 5).

Mueller et al. [34] also measured the isothermal He release from plutonia fuel pellets, nominally measuring 6-mm in diameter. The pellets were fabricated from oxalate fuel fired to a low temperature to form oxide fuel, then cold-pressed and sintered at 1900 K to 97–98% TD. The test specimens were aged at ambient temperature between

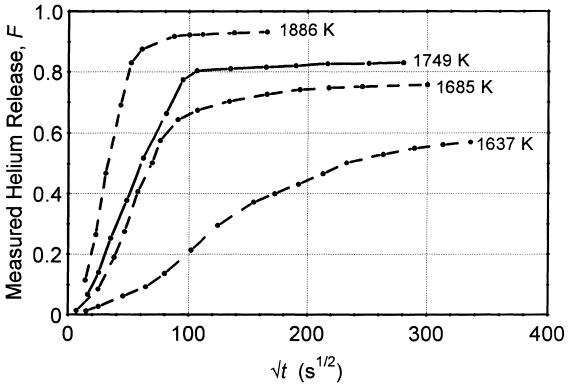

Fig. 5. Isothermal, fractional release of helium from 6-month-old $^{238}PuO_2$ fuel pellets of 87–88% TD [33].

~6 months and 2 yr, and then isothermally heated to 1273–1873 K for up to 12 h. Fig. 6 shows typical isothermal release fractions measured at constant fuel temperatures of 1670 and 1715 K. A release fraction of 0.50 was measured after 1.6 h at 1670 K, but only after ~10 min at 1715 K, and ~5 min at 1748 K [34]. In these experiments and the earlier isothermal helium release tests [33], more than 80% of the helium inventory in the fuel was released as the fuel temperature reached 1748 K.

The helium release data and the micrographic observations of Mueller et al. [34] agreed well with the release mechanisms delineated in Fig. 4 for helium in granular plutonia fuel. At temperatures <1273 K or after a very short time at higher temperatures, tiny (<1 μm in diameter) gas bubbles were formed along the grain boundaries. At higher temperatures, a more extensive network of intergranular bubbles, a few microns in diameter, had formed. Fig. 7 shows the micrographs of a 1-year-old fuel sample following isothermal heating at 1673 K. Note the as-fabricated round voids at the triple points between the grains. After 300 s at 1673 K, there were many strings of fine bubbles and some larger bubbles visible along the grain boundaries (Fig. 7(a)).

Further heating to higher temperatures produced large bubbles, often coalesced and spheroidized at the triple points, or formed very large, elongated (lenticular) bubbles along the grain boundaries (Fig. 7(b)). The coalescence of the small bubbles into larger ones often resulted in complete saturation of the grain boundaries. After 5 h at 1673 K, there were many large irregularly shaped bubbles along the grain boundaries, and almost no strings of small bubbles (Fig. 7(c)). Also, many of the grain boundaries were completely open.

4.3. Helium release during simulated re-entry heating experiments

Peterson and Starzynski [38] have subjected a LWRHU to a thermal ramp simulating atmospheric re-

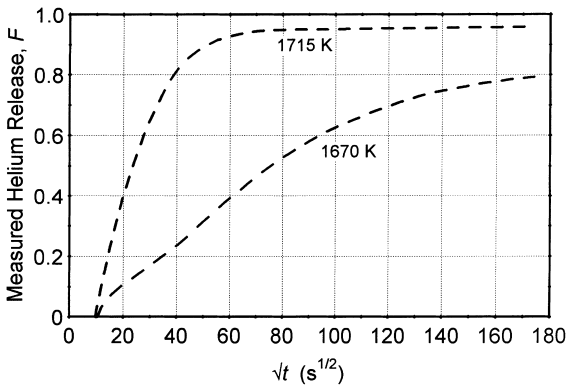

Fig. 6. Isothermal, fractional release of helium from 1-year-old $^{238}PuO_2$ fuel pellets of 97–98% TD fabricated from oxalate [34].

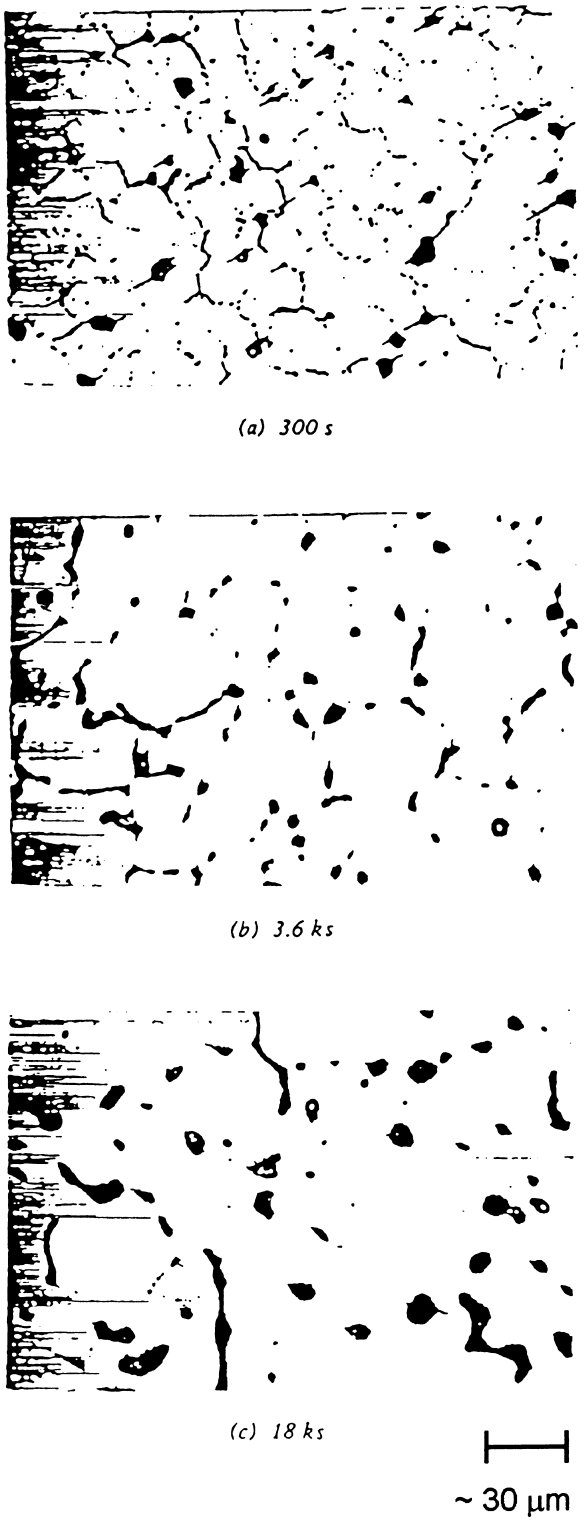

Fig. 7. Micrographs of 1-year-old plutonia fuel pellets during heating at 1673 K, showing growth and coalescence of intergranular bubbles: (a) after 300 s; (b) after 1 h; (c) after 5 h [34].

entry. The 7.93-year-old, $^{238}PuO_2$ pellet of the LWRHU had grain sizes of 7–12 μm and weighed 2.10 gm. The pellet was encapsulated in an iridium clad and contained within a graphite impact shell (LWRHU designated 027). The helium released from the fuel pellet passed through a vent assembly consisting of a frit (serving as a particulate filter) and a 0.6-mm-diameter orifice. The LWRHU was heated to 673 K and maintained at this temperature for 1 h, prior to performing the simulated re-entry heating experiment. The helium release was monitored as a function of temperature during the heating pulse (Fig. 8). The measured helium release rate was integrated as a function of time to obtain the helium release fraction from the pellet (Fig. 9). Post-test examination of the LWRHU and the fuel pellet revealed no evidence of fuel swelling or pellet damage. Based on the age and ^{238}Pu content (80 wt.%) in the fuel, a total of 8.46 std. cm^3 of helium were generated in the fuel pellet. Fig. 9 shows that as the pellet temperature reached 1723 K, 7.4 std. cm^3 of helium had been released from the fuel, which corresponded to a release fraction of 88%.

The results of Peterson and Starzynski [38] for the helium release in LWRHU during a re-entry heating pulse were consistent with the reported helium release in the experiments performed under isothermal heating conditions. Up to 20 s into the re-entry heating pulse, the fuel temperature remained below 900 K, and essentially no helium release was observed (Fig. 8). This corresponded to Region A in Fig. 4. Between 20–45 s, the helium release rate increased steadily, as the helium atoms were entrapped at the grain boundaries. The coalescence of intergranular bubbles to form open porosity increased the helium release (Region B in Fig. 4). At 45 s into the heating ramp, the fuel temperature reached ~1300 K and a transition occurred in the release rate (Fig. 8), indicating a burst release of helium. This rapid

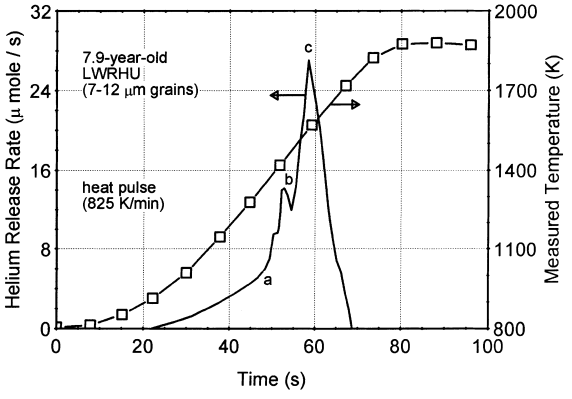

Fig. 8. Measured helium release rate and temperature during simulated re-entry heating pulse of 8-year-old LWRHU 027 [38].

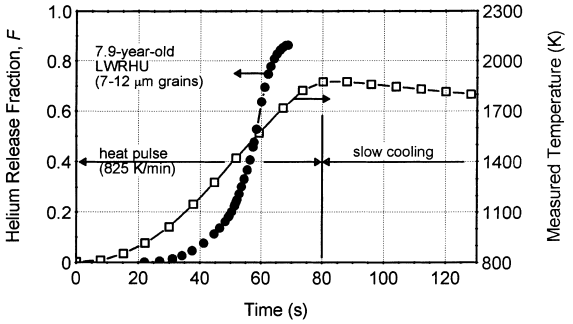

Fig. 9. Measured helium release fraction and temperature during simulated re-entry heating pulse of 8-year-old LWRHU 027 [38].

helium release is indicative of the formation of open porosity and grain boundary separation (Region C in Fig. 4). This release mechanism culminated at about 52 s when the fuel temperature was ~1400 K, at which the helium release rate reached a peak of ~15 μmol/s, which corresponds to the separation of the grain boundaries in the fuel. Subsequently, the helium release rate decreased, even though the fuel temperature continued to rise. At these temperatures, the rate of helium release was controlled by atomic and volume diffusion through the fuel grains (Regions D and E in Fig. 4). At about 60 s into the heating pulse, about 65% of the helium inventory were released from the fuel.

4.4. Helium release in polycrystalline fuel kernels

Data on helium gas release in polycrystalline PuO_2 fuel kernels are not available in the literature. However, post-irradiation heating tests of ZrC-coated, TRISO-type UO_2 particles have been performed at the Japan Atomic Energy Research Institute [10,11,39], to study fission products release. Minato et al. [11] have used fuel particles consisting of a dense (10 600 kg/m^3) UO_2 kernel (608 μm in diameter) which were fabricated by the sol–gel process. The particles have a low-density, 64-μm-thick PyC buffer layer (1110 kg/m^3), a 26-μm-thick, dense inner PyC layer (1840 kg/m^3), a 31-μm-thick ZrC layer (6600 kg/m^3), and a 55-μm-thick, dense outer PyC layer (1950 kg/m^3). The coated fuel particles were irradiated to a relatively low burnup of 1.5 at.% at a temperature of 1173 K. Optical and X-ray micrographs of polished sections of such particles showed the absence of grain boundaries in these polycrystalline kernels fabricated by sol–gel techniques. Fission gas release monitoring and X-ray micro-radiography revealed that no through-coating failure occurred during heating tests to 2073 K for 4 months and to 2273 K for 100 h. The release of short-lived noble gases was measured during irradiation.

After heating to 2073 K for 3000 h (4 months), signs of failure of the inner PyC coating (radial cracks) were observed in 10 out of 100 particles, and some degradation of the ZrC coating had occurred (1/4 of the thickness was attacked along the grain boundaries). After heating to 2273 K for 100 h, the inner PyC and the ZrC layer were damaged in most of the particles. The ZrC coatings were damaged due to the reaction between ZrC and the CO gas produced by the reaction of the PyC buffer layer and the oxygen liberated by fission in UO_2. This deterioration mechanism would not occur in coated, plutonia fuel kernels. The radioactive decay of ^{238}Pu atoms produces ^{234}U which remains in the stable oxide form. Therefore, the oxygen pressure in the fuel kernel would remain negligible and only small amounts of CO and CO_2 gases may be present in the particle.

Other ZrC-coated urania fuel particles were also irradiated to a higher burnup (4.0 at.%) and heat ramped to 2673 K [39]. The 8% ^{235}U-enriched UO_2 fuel kernels fabricated by the sol–gel process were 500–600 μm in diameter and had 96.6% TD. The ZrC coating was 31-μm thick, and the inner and outer dense isotropic PyC layers had a density of 1840 kg/m^3. In the ramp tests, only one out of 100 ZrC-coated TRISO fuel particles failed and released fission gases at 2673 K, whereas most of the SiC-coated TRISO particles had failed at that temperature [39]. The ZrC-coated TRISO UO_2 particles survived heating to 2673 K and the following observations were made: (a) large bubbles of fission-product gases existed within the oxide fuel kernel; and (b) the diameter increase of the particles was remarkably large: $22 \pm 3\%$, and surprisingly uniform.

Although the outer PyC layer itself could not contain the high internal pressure at such high strain, the ZrC layer of the particles remained intact after 100 min at 2673 K, and sustained major plastic deformation. The cross-sections of the ZrC-TRISO-coated fuel particles after heating to 2673 K for 100 min showed large fission gas bubbles distributed throughout the polycrystalline fuel kernels.

The results of the irradiation experiments of ZrC-coated UO_2 fuel particles indicated very low release-to-birth (R/B) rate ratios for noble fission gases ($<10^{-4}\%$) at temperatures as high as 2073 K [10,11]. Such low release fraction could be partially attributed to the low diffusion coefficient of noble gases in ZrC coating, and to the high gas retention in the fuel. The fuel kernels fabricated by sol–gel techniques consist basically of a polycrystalline structure with tiny enclosed porosity produced during the sintering process, and retain most fission gases either in the fuel matrix or in intragranular bubbles. The geometrical surface area of the fuel kernel would limit the release of the fission gases. This area remains essentially unchanged with increasing gas inventory and fuel temperature.

Helium gas release from polycrystalline $^{238}PuO_2$ fuel kernels fabricated by sol–gel processes is therefore expected to occur mostly by atomic and volume diffusion of helium in the fuel kernel. At relatively low temperature ($T < \sim 900$ K), helium is uniformly generated and distributed in the fuel in the form of dilute atoms, small atomic clusters or small as-fabricated voids, except near the surface. A fraction of the alpha particles emitted near the surface, within one range of the alpha particles in plutonia (~10–12 μm [40]), will escape the fuel, creating a small concentration gradient near the edge. This corresponds to Region A (Fig. 4) for the release of helium from granular plutonia fuel, and applies to all fuel forms indiscriminately.

Above 900 K, helium release in polycrystalline fuel kernels will continue to occur by atomic diffusion. Note that most of the helium gas inventory will be trapped and retained in gas bubbles within the fuel kernel. At much higher temperatures, one would expect an increase in the diffusion rate of helium, due to the increased mobility of the gas bubbles in the fuel and the continuation of atomic and volume diffusions. Nonetheless, the helium release fraction is expected to be much less than in small-grain plutonia fuel. Furthermore, the constraint imposed by the ZrC coating in coated plutonia particles would slow the release of He.

The next section presents a summary of the equivalent-sphere diffusion model for the release of noble fission gases and volatile fission products, and discusses the effects of the grain size and the decay constant (or half-life) on the release fraction of various radioactive species. The applicability of the results to predicting the release fraction of noble, non-radioactive gases, such as helium in plutonia fuel, is also discussed.

5. Equivalent-sphere diffusion model for noble fission gases and volatile fission products release

The equivalent-sphere model, originally proposed by Booth and Rymer [30], has been used to describe gas release from granular, oxide fuel in fission reactors [27–29] and granular plutonia pellets in GPHS and RHU units [16,33,34,37,38], respectively. The model assumes that the gas diffuses to the free surface of so-called equivalent spheres, from which it is readily released. The equivalent-sphere model has successfully been used to correlate gas-release experiments. The model treats granular fuel as a collection of equivalent spheres of uniform size, which have the same surface-to-volume ratio as the average release unit in the fuel matrix. Thus, the diameter of the equivalent sphere for gas release is $d = 2a = 6V/S_R$, where a is the sphere radius and V and S_R are the equivalent sphere's volume and surface area, respectively.

The total fuel surface area for the gas release, however, can be measured using gas-adsorption techniques, thus the effective value of d (or a) can be experimentally determined. When the average grain size of as-fabricated fuel is known, it may be substituted as an approximate value for d. The actual value of d, however, could be different, particularly as intragranular cracking occurs in the fuel, typically at temperatures <1400 K. Once the effective geometry of the fuel specimen for gas release has been characterized, the results of gas-release experiments can be used to determine the effective mass diffusion coefficient of the gases in the fuel matrix, D'.

5.1. Governing equations

In order to account for the effect of radioactive decay, the following diffusion equation:

$$\frac{\partial C}{\partial t} = \dot{B} + \frac{D}{r^2}\frac{\partial}{\partial r}\left(r^2\frac{\partial C}{\partial t}\right) - \lambda C, \tag{1}$$

is used to determine the release fraction, F, assuming an initial gas concentration $C(a,0) = 0$. In this equation, $\dot{B}$ is the production or birth rate of the gaseous isotope of interest and λ is its radioactive decay constant. The approximate solution of Eq. (1) for stable gases (i.e. when the third term on the right-hand side of Eq. (1) is zero) gives the release fraction, F as [30]

$$F \approx 6\sqrt{\tau/\pi}, \tag{2}$$

where $\tau = \int_0^t D'\,\mathrm{d}t$ is a dimensionless time, and

$$D'(T) = D(T)/a^2(T) \propto (S_R/V)^2 \times D. \tag{3}$$

In this equation, D', the effective diffusion coefficient (s^{-1}) depends on the release surface-to-volume ratio of the fuel and the mass diffusion coefficient of the gaseous species, D (m^2/s), which are both functions of the fuel temperature, T. The release fraction, F can be expressed in terms of the effective radius of the average release unit a, fuel temperature T, and release time t, as

$$F \propto \left(\frac{S_R}{V}\right) \times \sqrt{Dt} \propto \frac{1}{a(T)}T^{\gamma}\sqrt{t}. \tag{4}$$

As this equation indicates, F is inversely proportional to the effective radius of the average release unit in the fuel, and increases with the square root of time. Note that the fractional gas release, F, in Eqs. (2)–(4) is not equal to the release-to-birth rate ratio, $\dot{R}/\dot{B}$.

For radioactive fission gas species that have attained a steady-state concentration in the fuel, the fractional release, F^* equals in this case the release-to-birth rate ratio, and is given by [30]

$$F^* \equiv \dot{R}/\dot{B} \approx \left(\frac{S_R}{V}\right) \times \sqrt{\frac{D}{\lambda}} \propto \sqrt{\frac{D'(T)}{\lambda}} \propto \frac{1}{a(T)}T^{\gamma}\sqrt{T_{1/2}}. \tag{5}$$

This equation shows F^* to be inversely proportional to the average fuel grain size, a, and to increase with the square root of the half-life (or inversely proportional to the square root of the radioactive decay constant). As the half-life increases, F^* approaches the release fraction of non-radioactive species, given by Eq. (2). Thus, for the same fuel material, temperature, and grain size, F^* increases exponentially with the half-life of the gas species, approaching an asymptote. This conclusion is critical to the applicability of the release data of radioactive fission gases to the prediction of helium release in plutonia fuel particles, as detailed later.

The effective diffusion coefficient, D' increases exponentially with temperature and accounts for the increases in both the mass diffusion coefficient, D and in the effective release surface area, S_R (which includes fuel cracks and open grain boundaries) with temperature. Neglecting the as-fabricated open porosity, the surface-to-volume ratio of plutonia fuel microspheres for gas release can be expressed as

$$\left(\frac{S_R}{V}\right) = (1-\alpha)\frac{6}{d_p} + \alpha\frac{6}{d_g}, \tag{6}$$

where d_p is the fuel kernel diameter, d_g the grain size, and

$$\begin{aligned} &\alpha = 0 \quad \text{for } T \leqslant T_a \approx 900\ \text{K},\\ &0 < \alpha < 1 \quad \text{for } T_a < T < T_c \approx 1450\ \text{K},\\ &\alpha = 1 \quad \text{for } T \geqslant T_c \approx 1450\ \text{K}. \end{aligned} \tag{7}$$

The normalized surface area for helium gas release from plutonia fuel particles can thus be written as

$$\left(\frac{S_R}{S_p}\right) = (1-\alpha) + \alpha\frac{d_p}{d_g}, \tag{8}$$

where S_p is the geometrical surface area of the as-fabricated fuel particle.

5.2. Effect of fuel temperature on gas release

The effect of fuel temperature on the effective area for gas release in granular and polycrystalline fuels, S_R, is illustrated in Fig. 10. At temperatures below $T_a \sim 900$ K, gas release occurs by atomic diffusion from the fuel matrix, and S_R is equal to the geometrical surface area of the as-fabricated fuel sample (i.e. $\alpha = 0$). Between 900 K and $T_b \sim 1150$ K, $0 < \alpha < 1$ and S_R increases with temperature in granular fuel due to the formation and the coalescence of grain boundary bubbles. Above $T_b \sim 1150$ K, S_R increases rapidly with temperature as α

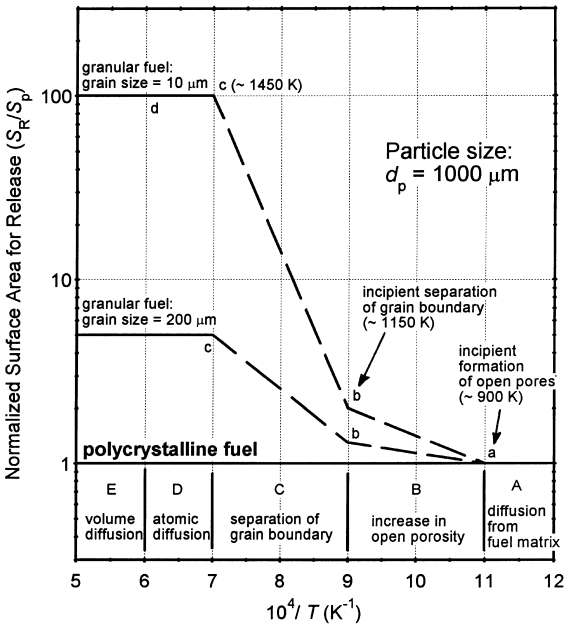

Fig. 10. Effective release surface area for gases in granular and polycrystalline fuels.

approaches unity, due to the formation of open porosity caused by the separation of the grain boundaries. At $T_c \sim 1450$ K, S_R reaches its maximum value and $\alpha = 1.0$, as the separation at the grain boundaries is complete. Above this temperature, the release fraction in granular fuel is no longer limited by the surface area available for release, but rather by the atomic and volume diffusion of the gases in the fuel grains (or the dependence of D on temperature). *It should be noted that the separation of the grain boundaries does not necessarily cause powdering of the fuel or breakup of its structure, but rather a full release of the gas at the grain boundaries through the formation of open porosity or networks of open tunnels.*

Fig. 10 illustrates the effect of the fuel grain size on S_R and potentially on the helium gas release in plutonia pellets or particles. For the same fuel temperature and particle geometry, increasing the grain size from a typical 10 to 200 μm could reduce the release fraction at high fuel temperatures (>1450 K) by more than an order of magnitude. As indicated earlier, a polycrystalline fuel kernel could be regarded as a single grain with a size equal to the kernel diameter. Thus, the effective surface area for gas release in a polycrystalline fuel particle would remain essentially unchanged and equal to the geometrical surface area of the particle. Therefore, the helium gas release in polycrystalline PuO_2 fuel would be expected to be significantly lower than in granular fuel pellets or microspheres.

To illustrate this point, consider a plutonia fuel microsphere that is 1 mm in diameter, at high temperatures >1450 K. A 200 μm grains fuel has a potential surface area for gas release that is five times that of a polycrystalline particle, while a 10 μm grain fuel particle would have 100 times the surface area for the helium release in a polycrystalline particle of the same diameter (Fig. 10).

Most of the gas release data reported in the literature for coated and uncoated fuel particles were for oxide fuels irradiated in fission reactors. However, in order to apply the reported fission gas release data to the helium gas release in plutonia fuel kernels, noble fission gas release measurements must be made at isothermal conditions, which is the case in plutonia fuel particles in RHUs and RPSs. Fortunately, such measurements have been made at the Berkeley Nuclear Laboratories (UK). The release fractions of radioactive, noble fission gases (Xe and Kr isotopes) and volatile fission products (Cs, I and Te isotopes) were measured for small-grain, large-grain and monocrystal UO_2 particles. The applicability of the reported noble fission gas release data to the He release in spherical plutonia particles operating at the same temperatures and having same microstructure is discussed next.

6. Isothermal release of noble fission gases and volatile fission products from granular and monocrystal UO_2 fuel particles

The only detailed studies of the isothermal release of noble fission gases and volatile fission products from granular and monocrystal fuel particles (Fig. 11) were those conducted at Harwell and at Berkeley Nuclear Laboratories in the UK [25–29]. These studies investigated the effects of grain size, radioactive decay constant, fuel burnup (up to 6.4 at.%) and temperature (up to 2023 K) on the release-to-birth rate ratio of the various gaseous and volatile isotopes. The temperature of the fuel particles during irradiation was kept nearly uniform, as would be expected during actual operation in fission reactors at low power density and in plutonia fuel particles in RHUs. UO_2 fuel microspheres consisting of small-grains (average grain size of 10 μm) (Fig. 11(a)) and large-grains (an effective grain size between 300 and 600 μm) (Fig. 11(b)) were irradiated up to a 6.4 at.% burnup. Monocrystal right cylinders of natural (0.72 wt.% ^{235}U) stoichiometric UO_2 were also irradiated (Fig. 11(c)). In addition, granular fuel specimens of 2.0% enriched UO_2 of near theoretical density, in the form of small cylinders, 10 mm long and 3 mm in diameter, having 7 and 40 μm grain sizes were irradiated [25].

During irradiation, the individual fuel particles were wrapped in tungsten mesh to prevent them from touching each other or the walls of the molybdenum container. The particles were irradiated isothermally in an electrically heated rig in the UKAEA reactor DIDO.

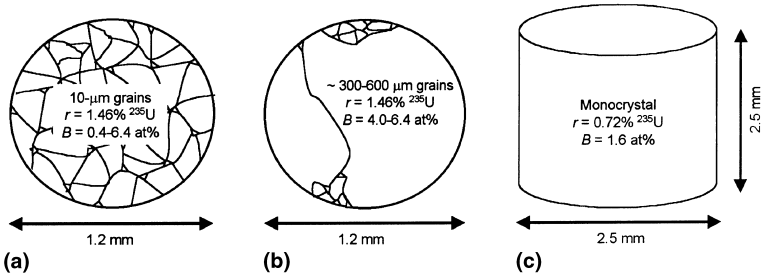

Fig. 11. UO_2 fuel samples used in isothermal gas release studies at Harwell and Berkeley Nuclear Laboratories [25–29]: (a) small-grain spherical particle; (b) large-grain spherical particle; (c) monocrystal right cylindrical particle.

Fission heating (thermal neutron flux of $\sim 2.6 \times 10^{17}$ m^2/s) produced a temperature drop between centerline and outer surface of the specimens of less than 100 K. The fuel particles were continuously swept with a He–2% and H_2 gas mixture to carry the released fission gases and volatile fission products. The volatile fission products were deposited on a cold finger while fission gases were collected using charcoal traps cooled with liquid nitrogen. The amounts of the various gaseous species released were measured by γ-spectroscopy, after correcting for their radioactive decay. The release rates of fission gases and volatile fission products were calculated based on these measurements, while their birth rates were calculated using computer codes [29].

6.1. Measured release data

Fig. 12 presents the measured release-to-birth rate ratios of ^{133}Xe, which has a half-life of 5.2 days, for the different fuel particles, as a function of irradiation temperature. The small-grain (10 μm) UO_2 microspheres released about 20 times more gas that the large-grain (~300–600 μm) ones. This ratio is comparable to that of the grain size ratio, consistent with Eq. (5), which predicts the release-to-birth rate ratio to be inversely proportional to the grain size. As expected, the monocrystal, natural uranium particles released less gas than the large-grain microspheres, due to the absence of grain boundaries in the former. However, the difference was not as large as might be expected. This is because the rate of fission was about half that in the large-grain fuel particles, due to the lower ^{235}U enrichment.

Figs. 12 and 13 show a change in the noble fission gas release-to-birth rate ratio in granular fuel particles at ~1350–1450 K, suggesting a change in the release mechanism. Below ~1100 K, the noble fission gases and volatile fission products diffuse to the grain boundaries, where they are trapped in the grain boundary bubbles or released by diffusion along the grain boundaries. Above ~1100 K, the growth and coalescence of intergranular bubbles cause separation of the grains, forming open porosity and effectively increasing the surface area available for release. This process continues with increasing fuel temperature up to ~1400 K. The increase in the release of the noble fission gas due to grain boundary separation would not occur in the monocrystal fuel particles, due to the absence of grain boundaries. This explains why release-to-birth rate ratio data for the monocrystal particles did

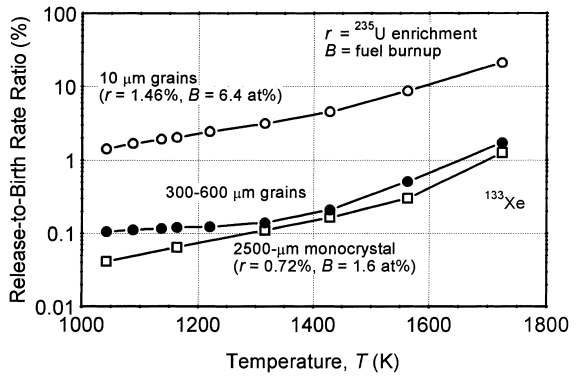

Fig. 12. Effect of grain size and temperature on isothermal release of ^{133}Xe ($T_{1/2} = 5.2$ days) in UO_2 fuel [25–29].

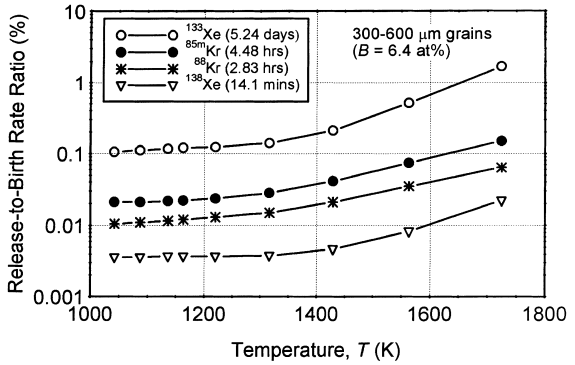

Fig. 13. Effect of half-life and temperature on isothermal release of noble fission gases from large-grain (~300–600 μm) UO_2 microspheres irradiated to a burnup of 6.4 at.% [25–29].

not exhibit a change in slope with increasing fuel temperature near 1400 K (Fig. 12). The increase in the release-to-birth rate ratios for granular and monocrystal particles at temperatures >1600 K is caused by the higher mobility of gas atoms and tiny intragranular bubbles in the fuel grains. The annealing of fission defects in the fuel matrix at such high temperatures could also have contributed to the increase in the mobility and the diffusion coefficient of fission gases, hence, increasing the gas release rate.

6.2. Effect of half-life on the release-to-birth rate ratio

The database showing the effect of half-life on the release of noble fission gases and volatile fission products from the large-grain (~300–600 μm) UO_2 microspheres is presented in Figs. 13–15 [25–29]. Gaseous radioisotopes decay as they diffuse through the fuel grains and are trapped at the grain boundaries for a period of time. Therefore, those having longer half-lives would exhibit higher release-to-birth rate ratios. According to Eq. (5), the release-to-birth rate ratio is proportional to the square root of the half-life, for the relatively short-lived isotopes that reach equilibrium early in time. Such dependence of the release-to-birth rate ratio on half-life is evident in Figs. 14(a) and 15 for the species having half-lives <10 days.

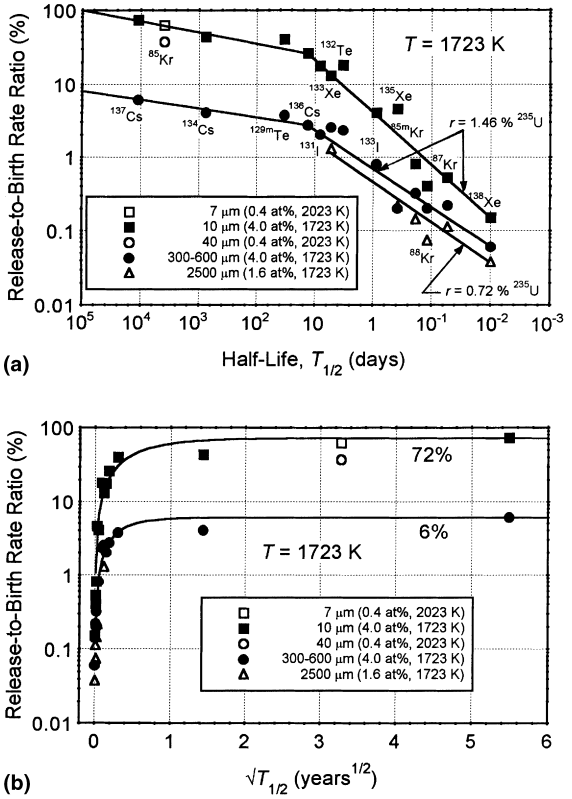

Fig. 14. Effects of half-life and fuel microstructure on isothermal release of fission gases and volatile products from UO_2 fuel samples irradiated at high temperature [25–29]: (a) versus the logarithm of the half-life; (b) versus the square root of the half-life.

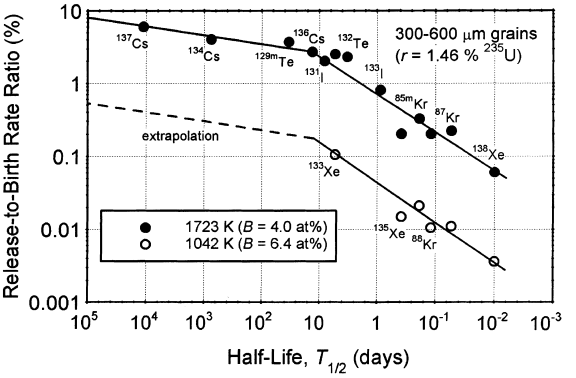

Fig. 15. Effects of half-life and temperature on isothermal release of fission gases and volatile products from large-grain (~300–600 μm) UO_2 microspheres enriched to 1.46% ^{235}U [25–29].

At 1723 K and 4.0 at.% burnup, the small-grain fuel particles (7–40 μm) released essentially all the noble fission gases and volatile fission products (~80% release), whereas only ~7% was released from the large-grain (~300–600 μm) fuel particles (Figs. 14 and 15). It is worth noting that the release fraction of the noble fission gases from the small-grain UO_2 particles is almost the same as that reported for granular plutonia pellets, of the same average grain size (7–12 μm), during re-entry heating tests to 1723 K [38]. When the data in Fig. 14(a) were plotted versus the square root of half-life, they exhibited an exponential increase with half-life, reaching asymptotic values at large half-life (Fig. 14(b)). These asymptotic values are representative of the release fractions of stable gases in granular UO_2 fuel during fission and of helium in plutonia fuel particles of the same average grain size.

Based on these experimental data, helium gas release from small-grain (7–40 μm) plutonia fuel at 1723 K would be ~80%, which is in agreement with the experimental data generated more than two decades ago at LANL for GPHS and LWRHU granular plutonia pellets [16,33,34,37,38]. For large-grain ($\geqslant$ 300 μm) and polycrystalline fuel microspheres, when heated up to 1723 K, the helium gas release could be more than an order of magnitude lower (~7%). The data presented in Fig. 14 are in excellent agreement with the theory (Eq. (5)), showing the strong effect of the grain size on $\dot{R}/\dot{B}$ of noble fission gases and volatile fission products, which is particularly evident for $T_{1/2} > 10$ days.

6.3. Effect of fuel temperature

The data presented in Fig. 15 illustrate the effect of fuel temperature on the isothermal release-to-birth rate ratios of the noble fission gases and the volatile fission products from the large-grain (~300–600 μm) UO_2 particles [25–29]. At 1042 K, only the data for the short-lived noble gases and volatile fission products were reported. This data were extrapolated to higher half-lives using a factor of three, which is the same as that for the high-temperature data between 10 and 10^5 days half-life (Fig. 15). This extrapolation is appropriate since the difference between the release-to-birth rate ratios of the radioactive and the stable gases equals the decay rate of the former, which is independent of temperature.

The data delineated in Fig. 15 indicate that at 1042 K, less than 1% of the noble fission gases and volatile fission products were released. Similar release fractions would be expected for helium gas in plutonia fuel particles having 300–600 μm grains. Also, since the nominal operating temperature in LWRHUs (~800 K) is several hundred degrees lower than 1042 K, the helium gas release at the operating temperature in coated particles of large-grain size ($\geqslant 300$ μm) plutonia fuel would be practically nil.

In summary, the isothermal release data of the noble fission gases and volatile fission products presented in this section for isothermally irradiated UO_2 fuel particles clearly demonstrated the strong effects of the fuel grain size and of the half-life on the steady-state release-to-birth rate ratios of the species. The data are consistent with the theory, Eqs. (4)–(8), particularly the dependence of $\dot{R}/\dot{B}$ on the half-life for the radioactive species that have attained equilibrium ($T_{1/2} < 10$ days). For the small-grain (7–10 μm) UO_2 fuel, the release-to-birth rate ratio of the long-lived noble fission gases and volatile fission products at 1723 K was nearly 80%. For the large-grain (~300–600 μm) fuel particles, the measured release-to-birth rate ratios at the same burnup of 4.0 at.% and fuel temperature of 1723 K were about an order of magnitude lower, ~7%, decreasing to <1% at a fuel temperature of 1042 K and higher burnup of 6.4 at.%. The release-to-birth rate ratios for both small-grain and large-grain UO_2 fuel particles increased exponentially with the half-life of the released species, as indicated by the theory (Fig. 14(b)).

6.4. Application to helium gas release in plutonia fuel kernels

The reported data for the isothermal release of noble fission gases and volatile fission products from granular fuel particles have provided a solid foundation for predicting the helium gas release in $^{238}PuO_2$ kernels, having similar grain size and as-fabricated porosity. The application of the reported data to helium release in plutonia particles includes a certain degree of conservatism. For example, the weakening of the grain boundaries by the bombardment of fission products, which could increase the release of the noble fission gases, does not occur in the α-emitter plutonia fuel. On the other hand, the micro defects in the fuel matrix caused by the fission fragments could serve as trapping sites, reducing the release rate of the noble fission gases. In addition, the constraint imposed by the ZrC coating could decrease the release of helium gas from the $^{238}PuO_2$ fuel kernels. Finally, due to the absence of grain boundaries, the helium releases in polycrystalline $^{238}PuO_2$ fuel kernels, fabricated using sol–gel techniques, might be significantly lower than in large-grain fuel kernels.

Based on the data reported by Harwell and Berkeley Nuclear Laboratories [25–29] for the isothermal release of noble fission gases and volatile fission products from small-grain, large-grain and monocrystal UO_2 fuel particles, the following conclusions pertaining to the helium gas release from plutonia fuel kernels can be drawn:

1. The helium gas release from small-grain (7–40 μm) plutonia fuel at 1723 K would be ~80%, decreasing to less than 10% at 1042 K. This conclusion is in agreement with the actual helium gas release data obtained at Los Alamos National Laboratory for GPHS and LWRHU plutonia pellets.
2. The helium gas release from large-grain ($\geqslant 300$ μm) plutonia fuel at 1723 K could be ~7%, decreasing to ~0.8% at 1042 K.
3. In polycrystalline plutonia fuel kernels fabricated using sol–gel processes, the helium gas release could be even lower than that for the large-grain $^{238}PuO_2$ kernels (i.e. <7% at 1723 K and <0.8% at 1042 K).

7. Summary and conclusions

The coated plutonia fuel particles have recently been proposed for potential use in future planetary exploration missions that employ radioisotope power systems and/or RHUs. The particles vary in size from 300 to 1200 μm and consist of a $^{238}PuO_2$ kernel with a thin (5 μm) PyC inner coating and a strong ZrC outer coating. The thickness of the ZrC is selected to ensure full retention of the helium gas generated by the radioactive decay of ^{238}Pu. The thickness of the ZrC coating, therefore, depends on the actual release fraction of the helium gas from the plutonia fuel particles during a simulated re-entry heat pulse, and on the fuel storage time (as much as 10 yr). During such transient heating, the fuel temperature could reach 1723 K, compared to ~800 K only during nominal operation. Reducing the thickness of the ZrC coating increases the $^{238}PuO2$ fuel loading in the coated particles, and, hence increases the specific thermal power of the RHU.

This paper reviewed the release mechanisms of helium in small-grain (7–40 μm) plutonia pellets currently being used in GPHS modules and LWRHUs, and in large-grain ($\geqslant 300$ μm) and polycrystalline plutonia kernels of the coated particles. The helium release mechanisms are similar to those of noble fission gases and volatile fission products from the UO_2 fuel particles, which were irradiated at isothermal conditions and had the same grain size and/or fuel microstructure. The applicability of these mechanisms to small-grain, large-grain and polycrystalline $^{238}PuO_2$ fuel particles was examined, and estimates of the helium release during a re-entry heating pulse up to 1723 K were presented. These estimates are based on the data reported by Harwell and Berkeley Nuclear Laboratories (UK) for the release of noble fission gases from granular and monocrystal UO_2 fuel particles, irradiated at isothermal conditions up to 6.4 at.% burnup and fuel temperatures up to 2030 K. The reported release fractions of the noble fission gases were consistent with the reported values of helium gas release in the tests performed at LANL using plutonia GPHS and LWRHU pellets of the same average grain size (7–40 μm). This agreement suggests that helium gas release in large-grain ($\geqslant 300$ μm) $^{238}PuO_2$ fuel kernels at 1723 K could be less than 7% and even lower in polycrystalline fuel kernels. At fuel temperatures $\geqslant 1000$ K, the He release would be nil.

Results indicated the need to fabricate $^{238}PuO_2$ fuel kernels that could retain most of the He generated by the ^{238}Pu radioactive decay, even at fuel temperatures as high as 1723 K. This is possible using large-grain ($\geqslant 200$ μm) or polycrystalline $^{238}PuO_2$ fuel kernels. The former could be fabricated using binderless agglomeration or similar processes while the latter could be fabricated using sol–gel or melting processes. Although these processes have successfully been used in the fabrication of UO_2 and mixed-oxide fuel kernels, they have not been demonstrated for the fabrication of $^{238}PuO_2$ fuel kernels.

Several remaining issues that are worthy of future investigations include:

1. Demonstrating the fabrication techniques of large-grain ($\geqslant 200$ μm) and polycrystalline plutonia fuel kernels and investigating the technical issues related to the application of the PyC and ZrC coatings using CVD processes.
2. Performing fracture impact tests and detailed analysis of the CPFCs to provide data to benchmark models. These data and the analysis results could also be used to guide the development and the selection of the appropriate graphite matrix material. Ultimately, mechanical, thermal, and aero-ablation testing of coated particle fuel in simulated accident environments will also be needed.
3. Performing helium gas release tests from large-grain and polycrystalline fuel kernels, both coated and uncoated, to confirm the current estimates and the release mechanisms.

Acknowledgements

This research was funded by Sandia National Laboratories (SNL), Kirtland Air Force Base, Albuquerque, NM, under Contract No. BE-2543, to the University of New Mexico's Institute for Space and Nuclear Power Studies. The opinions expressed in this paper are solely those of the authors. We are grateful to Dr Ronald J. Lipinski, SNL, and Mr Joseph A. Sholtis Jr., Sholtis Engineering & Safety Consulting, for their continuous technical support throughout this work effort.

References

[1] J.A. Sholtis Jr., R.J. Lipinski, M.S. El-Genk, in: M.S. El-Genk (Ed.), Proceedings of the Space Technology and Applications International Forum, STAIF-1999, American Institute of Physics, Woodbury, New York; AIP Conference Proceedings, 458 (Part 2) (1999) 1378.
[2] J.-M. Tournier, M.S. El-Genk, in: M.S. El-Genk (Ed.), Proceedings of the Space Technology and Applications International Forum, STAIF-2000, American Institute of Physics, Woodbury, New York; AIP Conference Proceedings, 504 (Part 2) (2000) 1458.
[3] D.J. Koeing, Los Alamos National Laboratory Report LA-10062-H, Los Alamos, NM, May 1986.
[4] L.L. Lyon, Los Alamos Scientific Laboratory Report LA-5398-MS, Los Alamos, NM, September 1973.
[5] E.K. Storms, D. Hanson, W. Kirk, P. Goldman, AIAA Paper No. 91-3454, September 1991.
[6] D.G. Pelaccio, M.S. El-Genk, D.P. Butt, Propulsion Power 11 (6) (1995) 1338.
[7] P.L. Allen, L.H. Ford, J.V. Shennan, Nucl. Technol. 35 (1977) 246.
[8] H. Huschka, P. Vygen, Nucl. Technol. 35 (1977) 238.
[9] W. Schenk, H. Nabielek, Nucl. Technol. 96 (1991) 323.
[10] K. Minato, T. Ogawa, K. Fukuda, H. Nabielek, H. Sekino, Y. Nozawa, I. Takahashi, J. Nucl. Mater. 224 (1995) 85.
[11] K. Minato, T. Ogawa, K. Fukuda, H. Sekino, I. Kitagawa, N. Mita, J. Nucl. Mater. 249 (1997) 142.
[12] R.C. Burnett, L. Bisdorff, J.R.C. Gough, Development of coated particle fuel – Part I: The fissile fertile particle, Dragon Project Report 151; also in: Proceedings of the Dragon Project Fuel Element Symposium, Bournemouth, England, 28–29 January 1963, CONF-630103-8, 1963.
[13] L.H. Ford, J.V. Shennan, J. Nucl. Mater. 43 (1972) 143.
[14] R.E. Latta, C.C. Browne, in: Proceedings of the Fifth Meeting of the Coated Particle Fuels Working Group on General Electric, Nuclear Materials & Propulsion Operation (GE-NMPO), CONF-273-2, Paper No. TM 63-6-7, June 1963.
[15] W.V. Goeddel, Nucl. Sci. Eng. 20 (1964) 201.

[16] P. Angelini, R.E. McHenry, J.L. Scott, W.S. Ernst Jr., J.W. Prados, Oak Ridge National Laboratory Report ORNL-4507, 1970.
[17] P.A. Haas, F.G. Kitts, H. Beutler, Chem. Eng. Prog. Symp. 63 (80) (1967) 16.
[18] R. Förthmann, G. Blass, J. Nucl. Mater. 64 (1977) 275.
[19] H. Lahr, Kerntechnik 19 (1977) 159.
[20] M.S. El-Genk, J.-M. Tournier, Final Report No. UNM-ISNPS-5-1999, Part I, Institute for Space and Nuclear Power Studies, The University of New Mexico, Albuquerque, NM, October 1999.
[21] J.F. Mondt, B.J. Nesmith, in: M.S. El-Genk (Ed.), Proceedings of the Space Technology and Applications International Forum, STAIF-2000, American Institute of Physics, Woodbury, New York; AIP Conference Proceedings, 504 (Part 2) (2000) 1169.
[22] A. Schock, in: Proceedings of the 16th Intersociety Energy Conversion Engineering Conference, American Institute of Aeronautics and Astronautics, Paper No. 819175, 1981.
[23] E.W. Johnson, Final Safety Analysis Report (FSAR) for the Cassini Mission, EG&G Mound Applied Technologies Report MLM-3826, UC-713, 1997.
[24] M.S. El-Genk, J.-M. Tournier, J.A. Sholtis Jr., R.J. Lipinski, in: M.S. El-Genk (Ed.), Proceedings of the Space Technology and Applications International Forum, STAIF–2000, American Institute of Physics, Woodbury, New York; AIP Conference Proceedings, 504 (Part 2) (2000) 1466.
[25] J.A. Turnbull, J. Nucl. Mater. 50 (1974) 62.
[26] C.A. Friskney, J.A. Turnbull, F.A. Johnson, A.J. Walter, J.R. Findlay, J. Nucl. Mater. 68 (1977) 186.
[27] J.A. Turnbull, C.A. Friskney, F.A. Johnson, A.J. Walter, J.R. Findlay, J. Nucl. Mater. 67 (1977) 301.
[28] J.A. Turnbull, C.A. Friskney, J. Nucl. Mater. 71 (1978) 238.
[29] C.A. Friskney, J.A. Turnbull, J. Nucl. Mater. 79 (1979) 184.
[30] D.R. Olander, Fundamental aspects of nuclear reactor fuel elements, Oak Ridge Report TID-26711-P1, US ERDA Technical Information Center, Energy Research and Development Administration, 1976 (Chapters 13–15).
[31] M.F. Lyons, R.F. Boyle, J.H. Davies, V.E. Hazel, T.C. Rowland, Nucl. Eng. Des. 21 (1972) 167.
[32] F. Scaffidi-Argentina, M.D. Donne, C. Ronchi, C. Ferrero, Fusion Technol. 32 (1997) 179.
[33] R.N.R. Mulford, B.A. Mueller, Los Alamos Scientific Laboratory Report LA-5215, 1973.
[34] B.A. Mueller, D.D. Rohr, R.N.R. Mulford, Los Alamos Scientific Laboratory Report LA-5524, 1974.
[35] C.C. Land, Los Alamos Scientific Laboratory Report LA-8083, 1980.
[36] A.W. Cronenberg, T.R. Yackle, EG&G Idaho National Engineering Laboratory Report No. NUREG/CR-0595, TREE-1330, R3, prepared for the US Nuclear Regulatory Commission and the US Department of Energy, 1979.
[37] D.E. Peterson, J.W. Early, J.S. Starzynski, C.C. Land, Los Alamos National Laboratory Report LA-10023, 1984.
[38] D.E. Peterson, J.S. Starzynski, Los Alamos National Laboratory Report LA-9226, 1982.
[39] T. Ogawa, K. Fukuda, S. Kashimura, T. Tobita, F. Kobayashi, S. Kado, H. Miyaniski, I. Takahashi, T. Kikuchi, J. Am. Ceram. Soc. 75 (11) (1992) 2985.
[40] D.E. Peterson, C.E. Frantz, Los Alamos National Laboratory Report LA-9227, 1982.